SPECIATION OF ANTIMONY IN ANCIENT TILE GLAZES: A *XAFS* STUDY

M.O. FIGUEIREDO[1,2], T. P. SILVA[1,2], J.P. VEIGA[2,1], J.P. MIRÃO[3] & S. PASCARELLI[4]

[1] Crystallography & Mineralogy Centre, IICT, Alameda D. Afonso Henriques 41-4º, PT-1000-123 Lisbon

[2] CENIMAT, Dept. Mater. Sci., New Univ. of Lisbon, PT-2829-516 Caparica

[3] Geophysics Centre, Univ. of Évora, Aptº 94, PT-7002-554 Évora

[4] ESRF, B.P. 220, FR-38043 Grenoble

14th ESRF Users Meeting
Grenoble, 8-13 February 2004

Introduction

The study of ancient decorative building materials with cultural value is a challenge to material scientists once it is usually necessary to apply only non-destructive techniques. Glazed tiles – *azulejos*, from the original Arab designation – have been used throughout the last five centuries in Portugal as decorative panels in the interior of private and public buildings.

To recover such artistic tile panels for exposure in a museum, not seldom the tile glaze has to be restored – a task requiring a concise knowledge of materials and colorants used at the time and place of tile production, so that only conformable new products are employed in tile restoration.

Yellow colouring in glasses & glazes is usually due to *antimony*, added mostly as lead antimonate [1]. However, as *the final form of Sb within the glaze is still questionable*, a *XAFS* study was undertaken on yellow tile glazes of Portuguese manufacture (XVII to XIX century).

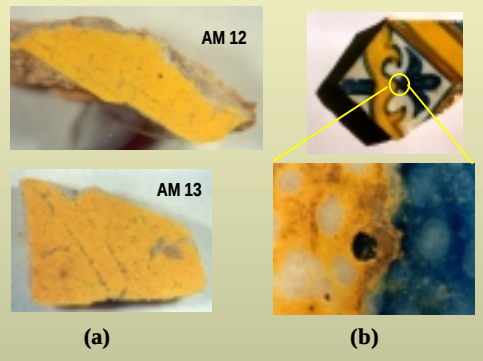

Fig. 1 – XVII century tiles, Portuguese manufacture. **(a)** studied fragments, magnified 20X (AM stands for "amarelo"/ yellow); **(b)** above, tile fragment in natural size; below, detail (50X) of assigned area.

Fundamentals

The *electron configuration* of **Sb** – [Kr] $4d^{10}\ 5s^2\ 5p^3$ – favours *formal valences* (3+) & (5+). The energy of ***K-absorption edge*** (ideally 30491 eV) will then display *shifts depending on the valence state(s)* present in the absorbing material.

The lone pair of electrons $5s^2$ – strongly localized in Sb^{III} – favours an asymmetric environment and unilateral positioning of ligands in Sb_2O_3 oxides. Simultaneously, the energy perturbation of $4d^{10}$ electrons due to chemical bonding in Sb^{V} is expected to induce *intensity variations* and/or *energy shifts* in XANES *post-edge details*.

A ***XANES*** study of ***Sb K-edge*** is therefore the clue for interpreting *antimony speciation* in a chemically complex material, particularly if suitable model compounds are available – namely, well crystallized minerals with known crystal structure.

Materials

Small fragments of glaze with an underlying thin layer of ceramic body (fig. 1) were directly irradiated. Model compounds – synthetic powders and slightly grinded *minerals* – were pelletized with BN. Selected minerals were: yellow ***cervantite*** (fig. 2) with Sb^{3+} in pyramidal (π_4) and Sb^{5+} in octahedral (o) coordination (with minor Ordoñezite, $Zn\ Sb_2\ O_6$); whitish minerals v***alentinite*** (fig.3) and ***senarmontite*** containing only pyramidal Sb^{3+}(fig. 4); and a poorly defined yellow mineral afine to pyrochlore, ***stibiconite***.

VALENTINITE

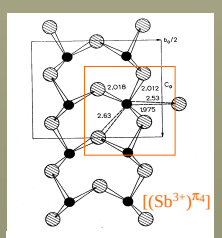

Fig. 3 – **Valentinite, Sb_2O_3 (orthorhombic** [6])

Fig. 2 – Layers of $[(Sb^{5+})^{o}\ O_6]$ octahedra in complex oxides: square (**Q**-type) in the minerals **cervantite** (tetragonal Sb_2O_4, [2]) and triangular (**T**-type) in **rosiaite** (trigonal $PbSb_2O_6$ [3]). The triangular octahedral layers are different in cubic pyrochlore-type oxides – the mineral **stibiconite** (ideally Sb_3O_6OH, never found well crystallized [4]) and allied synthetic oxides [5] (e.g. Sb_6O_{13}).

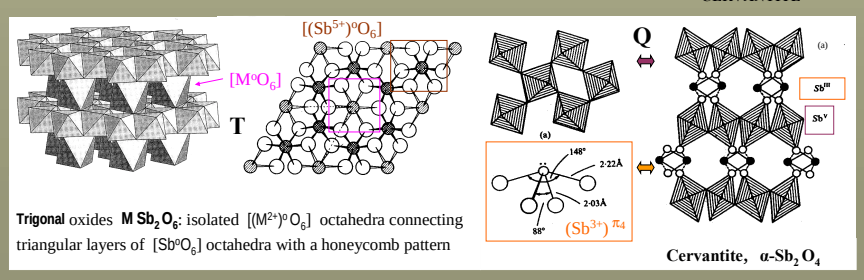

Trigonal oxides **$M\ Sb_2O_6$**: isolated $[(M^{2+})^{o}O_6]$ octahedra connecting triangular layers of $[Sb^{o}O_6]$ octahedra with a honeycomb pattern

Cervantite, α-Sb_2O_4

CERVANTITE

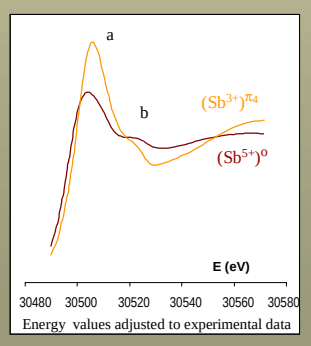

Energy values adjusted to experimental data

Fig. 5 – Contributions of the two ***Sb*** species to the calculated *K*-edge *XANES* spectrum of **cervantite** assuming a cluster of 87 atoms.

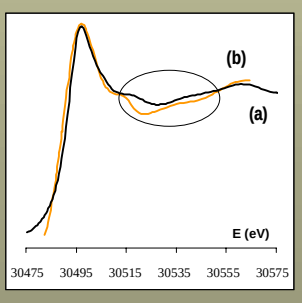

Fig. 6 – Sb *K*-edge *XANES* spectra of **valentinite:** (**a**) experimental (**b**) calculated for a cluster of 87 atoms. Assigned region clearly shows the presence of another phase in the mineral sample.

Experimental

The composition of mineral samples and synthetics used as model compounds was checked by X-ray diffraction, as well as the phase constitution of glaze fragments.

The instrumental set-up of BM-29 beamline at the ESRF was used to collect Sb *K*- edge *XANES* spectra in transmission mode.

To model the spectra, *ab initio* calculations were performed with the FEFF8.10 code [8] using a full multiple scattering approach.

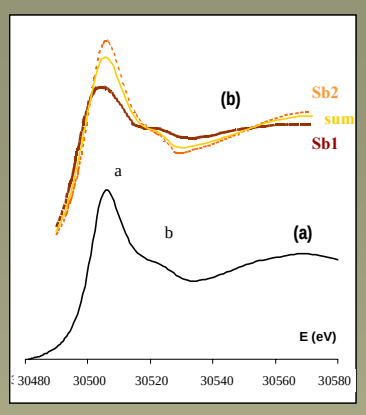

Fig. 7 – **Cervantite** Sb *K*-edge *XANES* : (**a**) sample containing minor Ordoñezite, experimental data; (**b**) calculated contributions assuming a cluster of 87 atoms and compound sum [Sb1+2Sb2].

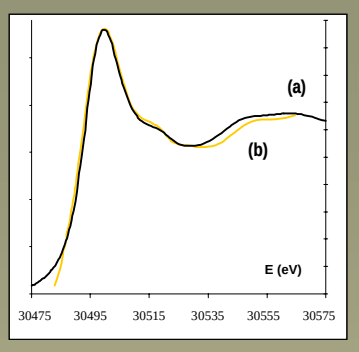

Fig. 8 – Sb *K*-edge *XANES* spectra of **stibiconite:** (**a**) experimental and (**b**) calculated assuming a cluster of 87 atoms and an atomic arrangement based on pyrochlore structure for an approximate formula Sb_4O_7.

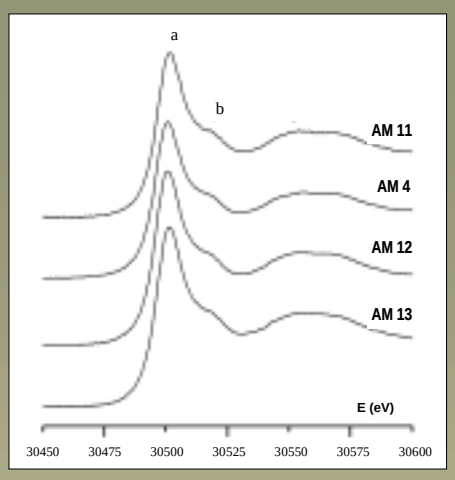

Fig. 12 – Experimental Sb *K*-edge *XANES* spectra of **yellow glazes,** XIX (**AM 11**) & XVII (**AM 4,12,13**) centuries. Edge energies vary

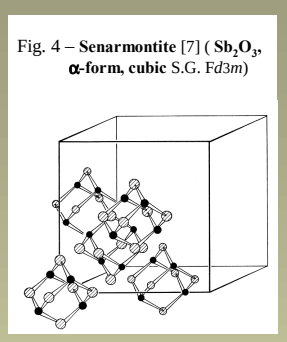

Fig. 4 – **Senarmontite** [7] (**Sb_2O_3, α-form, cubic** S.G. F*d*3*m*)

Fluorite-type arrangement in a cubic cell with packing vacancies and generation of Sb_4O_6 molecules

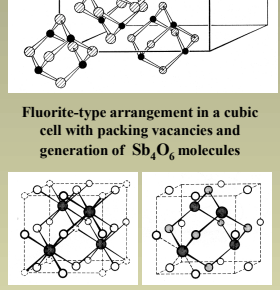

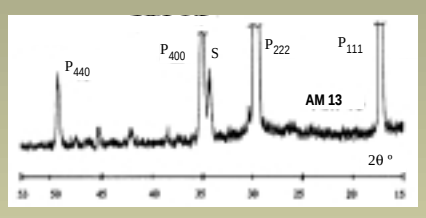

Fig. 9 – X-ray diffraction pattern (Cu Kα radiation) of glaze fragment **AM 13**: S, SnO_2 (cassiterite, opacifier) P, pyrochlore-type phase (strong lines are indexed).

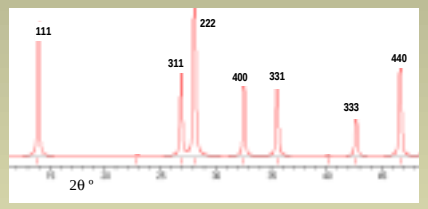

Fig. 11 – Calculated (PowderCell Program [10]) X-ray diffraction pattern (Cu Kα radiation) for an hypothetical pyrochlore phase (S.G. F*d*3*m*) with Sb^{5+} partially filling the octahedra (equipoint 16c) and Sb^{3+} occupying distorted pseudo-cubic sites (16d, fig. 10).

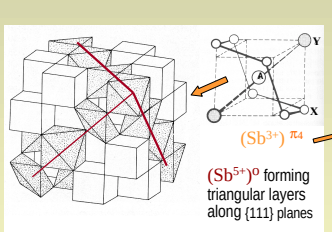

Fig. 10 – Ideal pyrochlore polyhedral arrangement derived from a fluorite-type anionic close packing

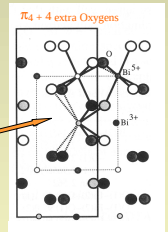

From reference [9] on Bi_2O_4 monoclinic, isostructural with β-Sb_2O_4

Yellow Sb-oxides with atomic arrangement derived from pyrochlore

(*e.g.*, "giallo di Napoli" and the poorly defined mineral *Stibiconite*)

Conclusions & Comments

Sb^{5+} & ***Sb^{3+}*** have *distinct coordination tendencies in crystalline solids* (fig. 2). Therefore, Sb *K*-edge details (a & b) allow to distinguish between chemical species (fig. 5).

Speciation of *fuser metals* and *colorants* in ancient tile glazes and glasses enlightens chemical affinities and correlations in phase behaviour that can account for ageing mechanisms. The *mineral world* may additionally provide *useful suggestions*.

The *energy shift* (4 eV) observed for the absorption edge in *glaze fragments* indicates the presence of both Sb species (3+ & 5+). Combined with X-ray diffraction data, this result clearly shows that the *yellow colour* obtained by adding lead antimonate as raw material is due to the presence of ***Sb^{5+}*** hosted by a *dispersed nanophase with pyrochlore structure* (figs. 9 to 11). Indeed, the species ***Sb^{3+}*** gives no colour to natural compounds and is recognized as a network-forming cation in oxide glasses [11].

There is a remarkable coincidence between calculated Sb *K*-edge *XANES* and data collected from controlled model minerals (e.g., fig. 8). The observed differences are mainly due to minor contaminant phases (as in valentinite sample, fig. 6).

References

[1] WAINWRIGHT, I.M. *et al.* (1994) Lead antimonate yellow. In *Artists Pigments: A handbook of their history & characteristics.* Editor R. Feller, Nat. Gallery of Art, Oxford Univ. Press.

[2] THORNTON, G. (1977) A neutron diffraction study α-Sb_2O_4. *Acta Cryst.* B33 1271.

[3] BASSO, R. *et al.* (1996) Rosiaite, $PbSb_2O_6$, a new mineral from the Cetine mine, Siena, Italy. *Europ. J. Miner.* 8 487.

[4] MASON, B. & VITALIANO, C.J. (1952) The mineralogy of the antimony oxides &antimonates. *Min. Mag.* 94 100.

[5] STEWART, D.J. *et al.* (1972) Pyrochlores. VII. The oxides of antimony: an X-ray and Mössbauer study. *Canad. J. Chem.* 50 690.

[6] SVENSSON, C. (1974) Crystal structure of orthorhombic antimony trioxide, Sb_2O_3. *Acta Cryst.* B30 458.

[7] *Strukturbericht*, Band I (1913-1928) 245.

[8] ANKUDINOV, A. *et al.* (2000) Manual of FEFF8.10 program. *The FEFF Project.* Dept. Physics, Univ. Washington, Seattle/USA, 62pp.

[9] KUMADA, N. *et al.* (1995) Crystal structure of Bi_2O_4 with β-Sb_2O_4 – type structure. *J.Solid St. Chem.* 116 281.

[10] KRAUS, W. & NOLZE, G. (1996) POWDER CELL – A program for the representation and manipulation of crystal structures and calculation of the resulting X-ray powder patterns. *J. Applied Cryst.* 29 301.

[11] ELLISON, A.J.G. & SEN, S. (2003) The role of Sb^{3+}as network-forming cation in oxide glasses. *Phys.Rev.* B67 5223.